

The role of surface texture and anode-cathode size ratios on mass transfer in undivided electrochemical reactors

H. HAMZAH

Department of Chemistry, Salford University, Salford, UK

A. T. KUHN

Department of Bio-Materials Science, Institute of Dental Surgery, 256 Gray's Inn Road, London WC1, UK

Received 19 September 1979

The performance of undivided cells with disparate anode-cathode ratios was studied using cerium(IV) reduction as a test reaction. The effects of electrode material and surface texture are reported. Results have been fitted to a computer-based model, and the role of bubble evolution and electrode coverage by bubbles is considered. Results are contrasted with those of a similar study using hypochlorite formation, which can give qualitatively different results.

1. Introduction

It is commonly agreed that electrochemical processes in undivided cells operate at considerably less than theoretical current efficiency, for the simple reason that species produced at one electrode may be destroyed at the other. Thus in the electrolysis of brine, chlorine formed at the anode can migrate in the form of hypochlorite and be reduced. The conventional solution to this problem is to interpose a diaphragm or membrane between the anode and cathode, thus preventing (ion-exchange membrane) or restricting ('filtering diaphragm') the back-reaction of the species formed at each electrode. There is a second approach, indeed one that has been known for many years. This is to use a cell with disparately sized anodes and cathodes, so that species formed, for example, at a large anode, are prevented from being once more reduced by employment of a small cathode. In the earliest times, it was thought that a ratio of anode-to-cathode of say 10:1 would be reflected in the efficiency with which such a cell operated. In fact this was not so and such cells were much less efficient than this simple theory suggested. The surprising fact is that there appears to be an almost total dearth of data describing the quantitative behaviour of undivided cells. We have only managed to locate one example.

In the work of Divin [1] the effect of cyanide oxidation was studied using undivided cells with large planar anodes and small area wire cathodes. Anode-to-cathode ratios of 1:1, 1:4 and 1:16 were used and the concentration of CN^- was nearly ten times lower in the latter case because of the reduced amount of CNO^- reduction to CN^- at the cathode. We might also cite two US patents [2, 3] showing that current efficiencies of 80-90% can be achieved with undivided cells having anode-to-cathode ratios from 40:1 to 400:1.

It is axiomatic that the current density at anode and cathode in such cells must differ. And since the intention is that at one electrode, the total current density must exceed the limiting current density of the process one is trying to restrict, it follows that a second electrode process must be taking place there. Almost without exception, this process involves gas evolution (hydrogen or oxygen evolution) and as Ibl [4, 5] and many subsequent workers [6-13] have shown, this enhances the mass-transfer of the first reaction and thereby seeks to defeat the objective of the cell design as first described. Nevertheless, a net benefit does remain, and cells with disparate electrode sizes are more efficient than their symmetrical analogues. In terms of this, it follows that any investigation of an undivided cell

with disparate electrode sizes must take into consideration the enhancement of mass transport due to gas evolution. A second problem, which occurs in all electrode processes, relates to electrode roughness or texture. Here again, the literature is very sparse. Ibl *et al.* [4] have studied the effect of bubble evolution on the mass transfer rate of a redox process as a function of surface roughness, but in a static (i.e. no forced convection) system. They found no significant effects. In this way they are somewhat at variance with Fouad *et al.* [9]. We have examined the effect of surface roughness in a pumped undivided hypochlorite cell and find there a very considerable effect [14]. In this paper, both factors will be explored by studying the reduction of Co(IV) at cathodes of various surface areas (relative to anode area).

2. Experimental

We considered various designs for undivided cells with disparate anode-to-cathode ratios. It was thought essential to maintain the best possible potential and current distribution, and this ruled out many designs which have occurred in the literature. The obvious design is the concentric cell. Alternatively, we have the parallel plate planar cell in which the overall dimensions of anode and cathode are substantially the same, but where the true area of one has been reduced by blanking off areas. Both designs were used here. In the latter, it was decided that the maximum diameter of the blanked-off areas should

not, in the interests of preservation of good potential distribution, be greater than the inter-electrode gap. The concentric cell is shown in the diagram (Fig. 1). Ibl and co-workers suggested masking off the electrode with perforated materials, and have more recently published a most important paper in which results are given for electrodes covered with more or less porous materials such as polypropylene, etc. There is no doubt that their ideas in this respect will be more or less widely adopted.

2.1. Test reaction

The two standard test-reactions are the ferri-ferrocyanide redox couple or the ceric-cerous couple. Ibl *et al.* [20] have criticized the first of these because the electrode can be passivated and so lead to erroneous results. The latter was thus exclusively used.

2.2. Cell design

Two types of cell design were used in this work. A parallel plate cell of the same design as that described previously [15] in which rectangular electrodes were inlaid into a channel section in the cell. The anode-to-cathode ratio was varied only to a very slight extent by use of one electrode of greater overall dimensions than the other. Rather, the ratio of anode-to-cathode areas was varied by drilling holes in one electrode at regular intervals, then filling these with epoxy-resin and

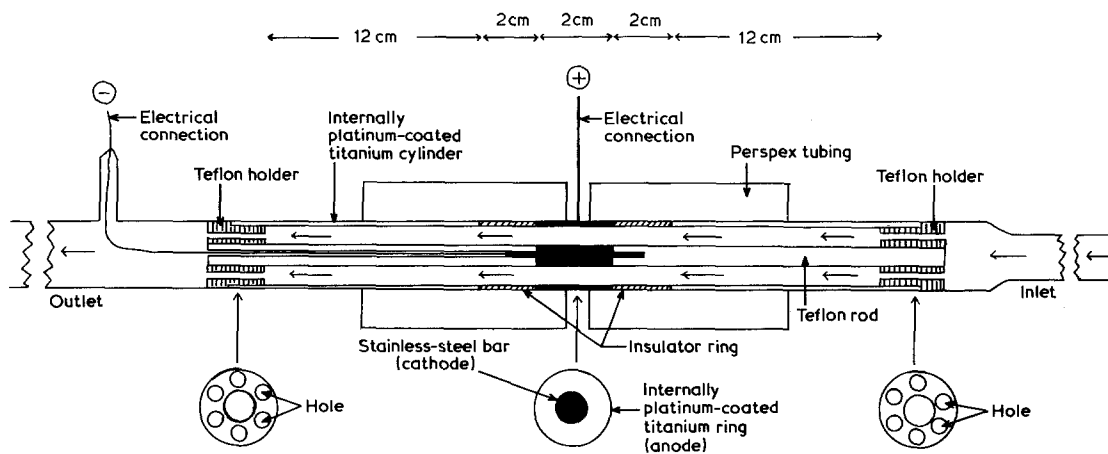


Fig. 1. A sketch of the concentric cell.

Table 1. Details of anode-to-cathode ratios used in the parallel plate cell

	Overall size (cm X cm)	Exposed area		
		1 cm ²	2 cm ²	2 cm ²
Anode (A)	6.6 X 3.0	19.8	19.8	19.8
Cathode (C)	7.6 X 3.4	25.8	17.4	10.9
A:C Ratio	—	0.76:1	1.14:1	1.81:1

smoothing the entire surface of the electrode. Even using this method, an anode-to-cathode ratio of 1.8:1 was the largest we could obtain without inducing a situation where substantial inequalities of current distribution might occur, that is to say geometries where the inter-electrode gap was substantially less than the diameter of the insulating circles on the electrode. Details of the overall sizes and exposed areas are given in Table 1.

The second cell employed was based on the concentric cylinder design. Inherently, this is much better suited to disparate anode-to-cathode area ratios. The anode was a tube of Ti, Pt-plated on the inside face. The cathode was a cylinder threaded through the tube. The area of the cathode could be reduced by using a thinner cylindrical section. At the point when even this approach threatened to cause problems of poor current distribution etc., a further idea was employed, namely to mill wide grooves into the cylindrical cathode and fill these with epoxy-resin, again smoothing out the entire surface after setting.

The anode-cathode assembly as described above, was mounted into perspex tubing, with 14 cm smoothing sections upstream and downstream of the electrodes. The Ti tube was recessed into the perspex so that the surface was perfectly flush and smooth. The cathode was fitted into a PTFE rod of the same diameter as the

metal itself, and electrical connections were made through the interior of the PTFE to the metal. This composite assembly was supported by two discs, one at each end of the cylindrical cell-housing. These discs were perforated to provide the minimum possible resistance to flow, and the void between the discs and the electrode was packed with short sections of glass tubing, aligned to the axis of flow, to effect the best possible smoothing of the flow. The cell is depicted in Fig. 1.

The hydrodynamics of this cell were tested by injection of a strongly coloured solution into the flowing system which was circulated at the rate used in this work. The flow was observed with a closed-circuit TV and also with a cine-camera. No evidence of turbulent flow was observed.

1.3 l of Ce(IV) (SLR) solution (0.01 M) were circulated through the cell with an Iwaki magnetic pump and maintained at 23° C using a water-bath and coil. All runs were begun by filling the reservoir with the Ce(IV) solution, and the build-up of Ce(III) was followed as a function of time. The concentration of Ce(IV) was determined by titration with Fe(II) [6] and the concentration of Ce(III) was then calculated by subtracting the concentration of Ce(IV) from its initial concentration. Control experiments showed that in the absence of applied voltage, there was no loss of Ce(IV) with time. Using this design, experiments were conducted under the conditions shown in Table 2.

3. Results and discussion

The results are shown in Figs. 2-8.

It is clear from the results that diminution of anode-to-cathode ratio does in general have an

Table 2. Summary of experimental conditions for Ce(IV) reduction

Conditions	Parallel plate cell	Concentric cell
Current (A)	0.2, 0.1, 6.0	0.15, 0.75, 4.5
Anode current density (mA cm ⁻²)	10, 50, 300	10, 50, 300
Temperature (° C)	23 ± 1	23 ± 1
Flow-rate (cm s ⁻¹)	70	28
Reynolds number	3500	3500
Anode area (A) (cm ²)	19.8	15.1
Cathode area (C) (cm ²)	25.8, 17.4, 10.9	6.1, 3.05, 1.4
A:C ratio	0.76:1, 1.14:1, 1.8:1	2.5:1, 4.9:1, 10.6:1

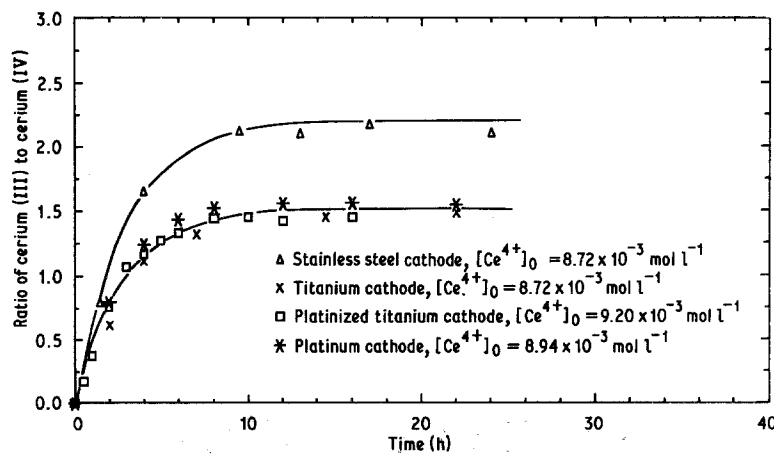
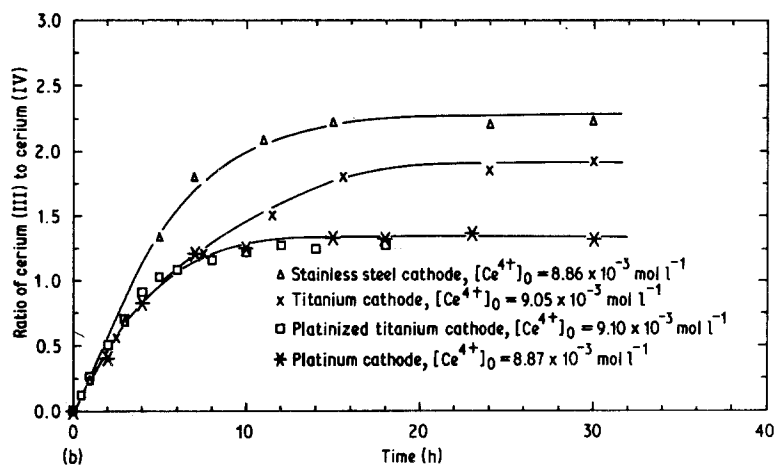
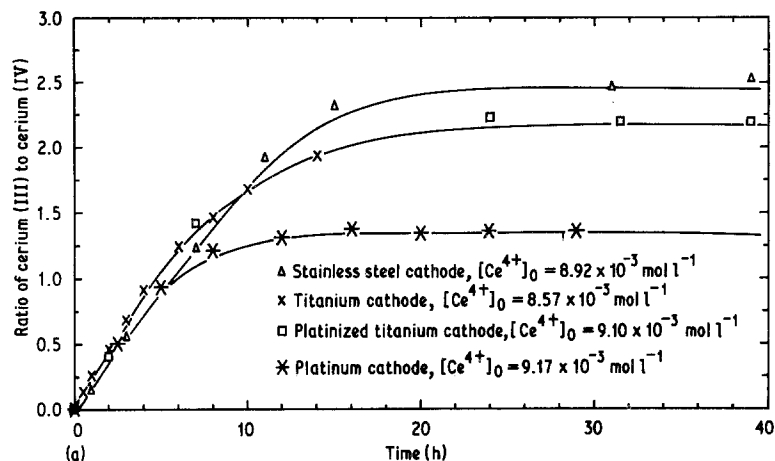


Fig. 2. Ratio of Ce(III) to Ce(IV) versus time for electrolysis of Ce^{4+} solution using various cathode materials at anode current densities of (a) 10 mA cm^{-2} ; (b) 50 mA cm^{-2} and (c) 300 mA cm^{-2} . ($T = 23 \pm 1^\circ \text{ C}$, $N_{Re} = 3500$).

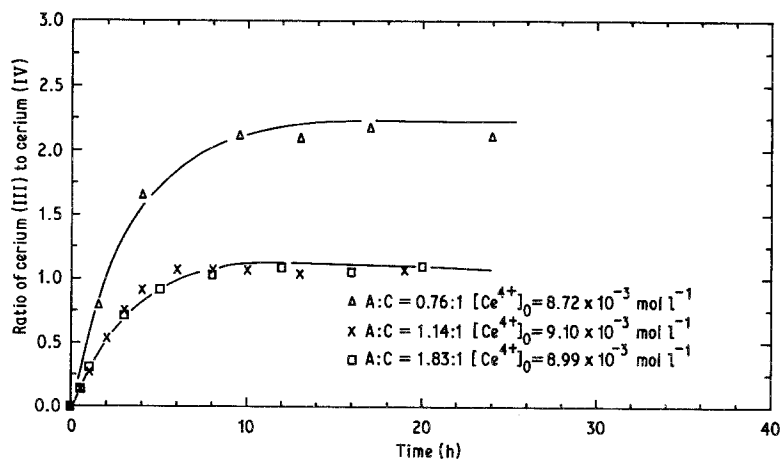
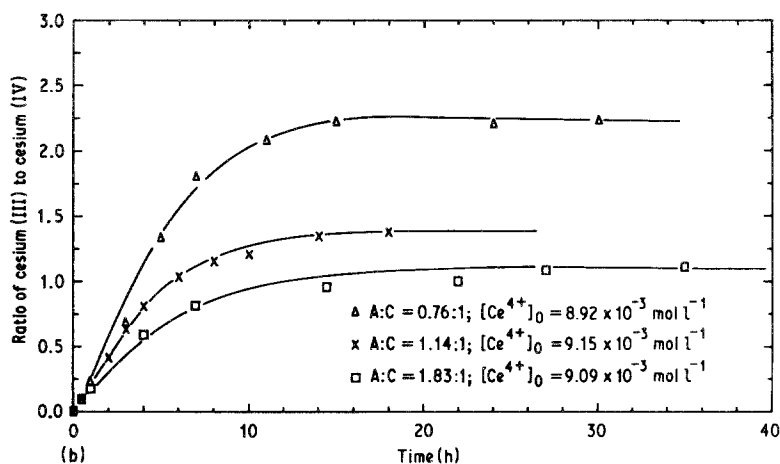
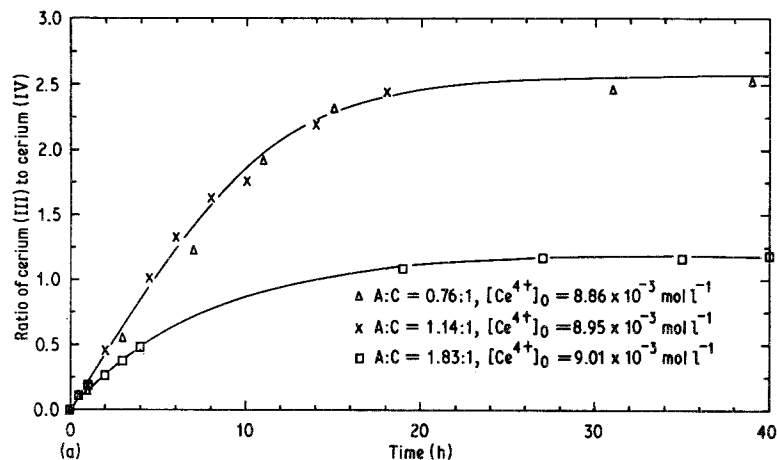


Fig 3. Ratio of Ce(III) to Ce(IV) vs time for electrolysis of Ce^{4+} solution using stainless steel cathodes of different anode-to-cathode ratios at anode current densities of (a) 10 mA cm^{-2} ; (b) 50 mA cm^{-2} and (c) 300 mA cm^{-2} . ($T = 23 \pm 1^\circ \text{ C}$, $N_{Re} = 3500$).

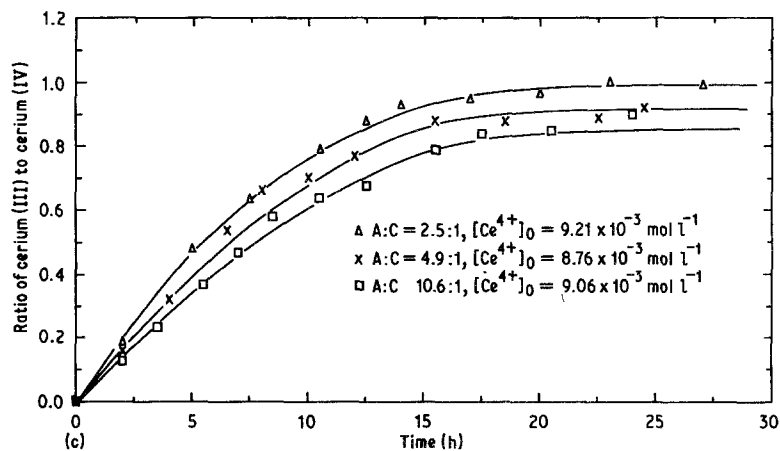
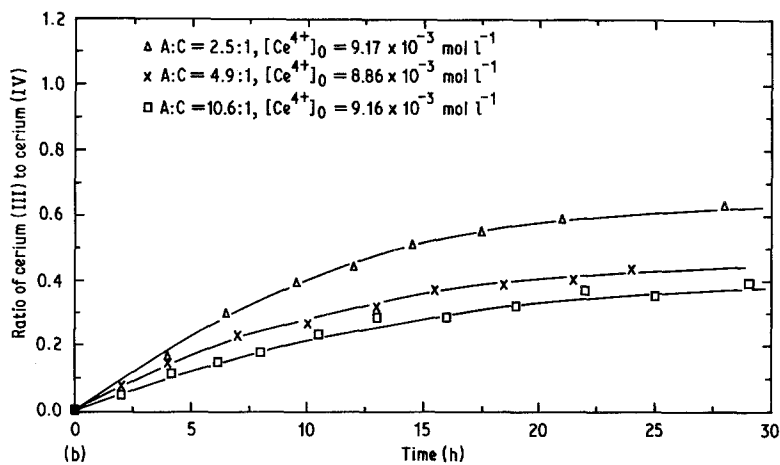
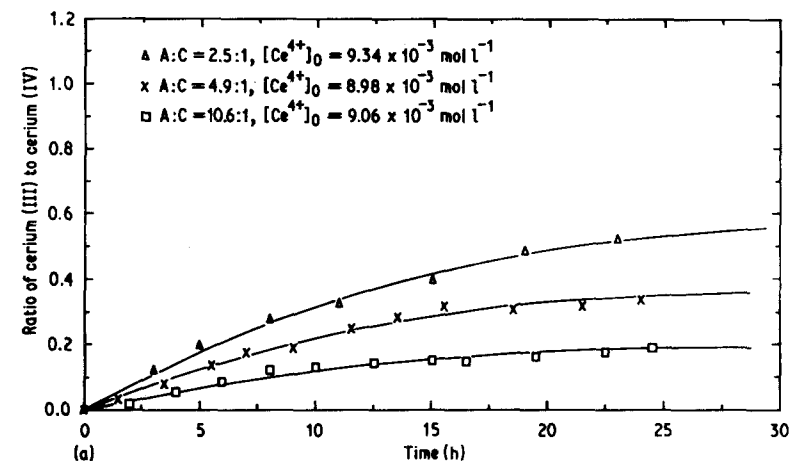


Fig. 4. Ratio of Ce(III) to Ce(IV) versus time for electrolysis of Ce^{4+} solution in concentric cell using stainless steel cathodes of various anode-to-cathode ratios at anode current densities of (a) 10 mA cm^{-2} ; (b) 50 mA cm^{-2} and (c) 300 mA cm^{-2} ($T = 23 \pm 1^\circ \text{ C}$, $N_{\text{Re}} = 3500$).

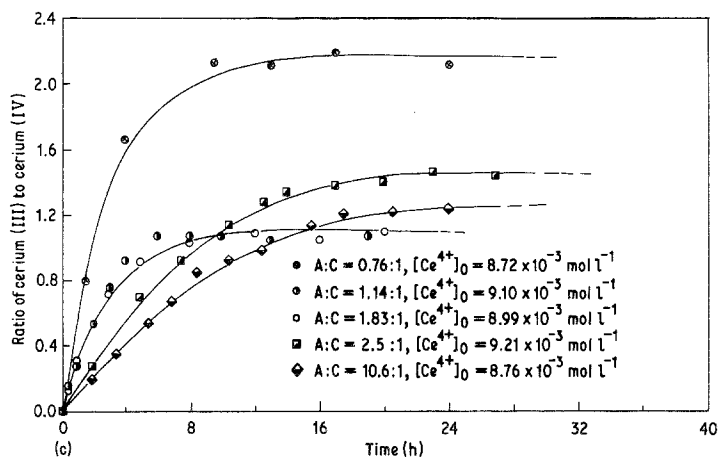
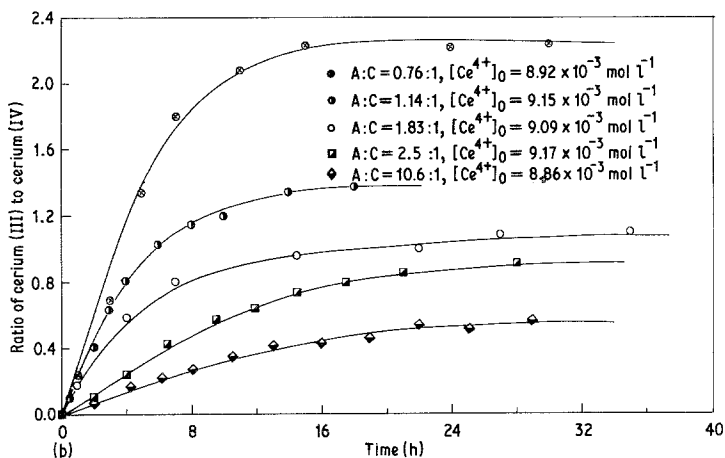
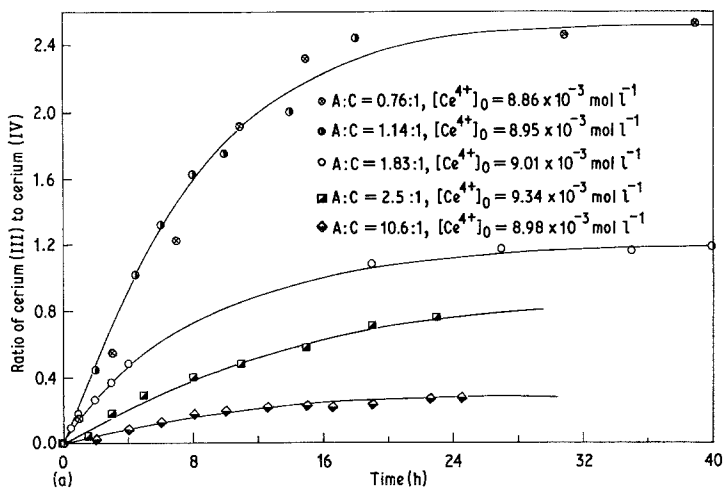


Fig. 5. Normalization of the results from concentric cell to parallel plate cell for electrolysis of Ce^{4+} solution. Anode current densities: (a) 10 mA cm^{-2} ; (b) 50 mA cm^{-2} ; and (c) 300 mA cm^{-2} .

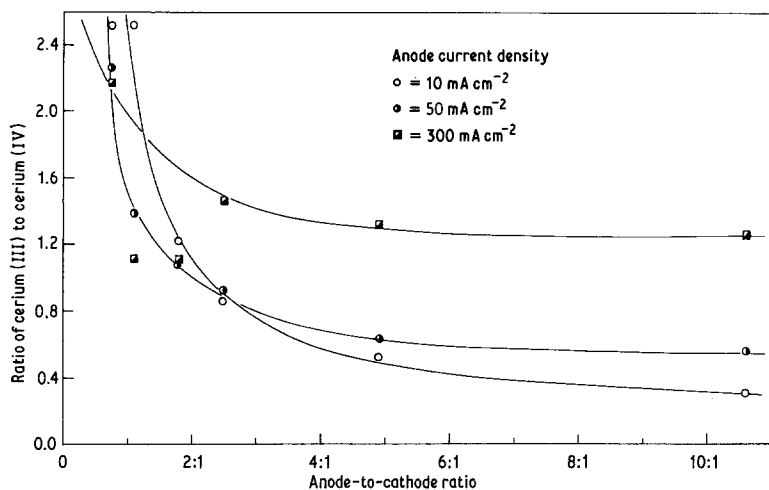


Fig. 6. Ratio of Ce(III) to Ce(IV) at infinity (R_∞) versus anode-to-cathode ratio at different current densities.

effect on the rate of the back-reaction. Our first concern was to compare the results from the two cells to see to what extent design is an independent variable. The results [Ce(III):Ce(IV) versus time] from one cell (the concentric cell) were normalized to the other, to account for the slight difference in volume of electrolyte used, and also the differences in electrode area. Thus runs made at the same current density were normalized on the ratios of the two electrodes used. The results are seen in Fig. 5.

Our second aim was to see whether these results could be 'modelled' in the same way as Heal *et al.* [15] had earlier modelled hypochlorite build-up using a computer-based model. In this, there are two tests one can apply. In the simplest case, one seeks merely to predict the ratio of Ce(III):Ce(IV) at infinite time. The equation used to represent this was simply:

$$I_{\text{net}} = \text{rate of reduction of Ce(IV)} \\ - \text{rate of re-oxidation of Ce(III)} = 0.$$

Theoretical values in Table 3 were calculated using the equation

$$I_{\text{net}} = \frac{nFD_1A_c(1-\theta_c)[\text{Ce}^{4+}]}{\delta_c} \\ - \frac{nFD_2A_a(1-\theta_a)[\text{Ce}^{3+}]}{\delta_a} = 0$$

From Fig. 6 it is seen that an increase in anode-to-cathode ratio does minimize the amount of back-oxidation of Ce(III) to Ce(IV) but as the current

density is increased this tendency is at least partly defeated. We can explain this in terms of back-mixing promoted by vigorous gas evolution at both anode and cathode.

The more difficult task is to model the entire process, from $t = 0$ to $t = \infty$.

The calculated R [Ce(III) to Ce(IV)] versus time plots were computed using the equation

$$I_{\text{net}} = \frac{nFD_1A_c(1-\theta_c)[\text{Ce}^{4+}]}{\delta_c} \\ - \frac{nFD_2A_a(1-\theta_a)[\text{Ce}^{3+}]}{\delta_a}$$

and in the iteration the value of [Ce(IV)]_{*t*} at time *t* was obtained by subtracting [Ce(IV)] being reduced at time *t*, from its initial concentration, i.e.

$$[\text{Ce(IV)}]_t = [\text{Ce(IV)}]_{t=0} - [\text{Ce(III)}]$$

and

$$[\text{Ce(III)}] = \frac{I_{\text{net}}t}{nFV}$$

It will be seen that we have based our equations on the model of Beck [17]. We might equally well have used the more recent model of Vogt [18] and indeed, this has been done using other reaction systems by one of us [14]. However, it has been found that the differences between the two models are not significant in the context of other unknowns.

Fig. 7 shows that extremely good agreement can be obtained between experimentally-obtained and theoretically-derived data.

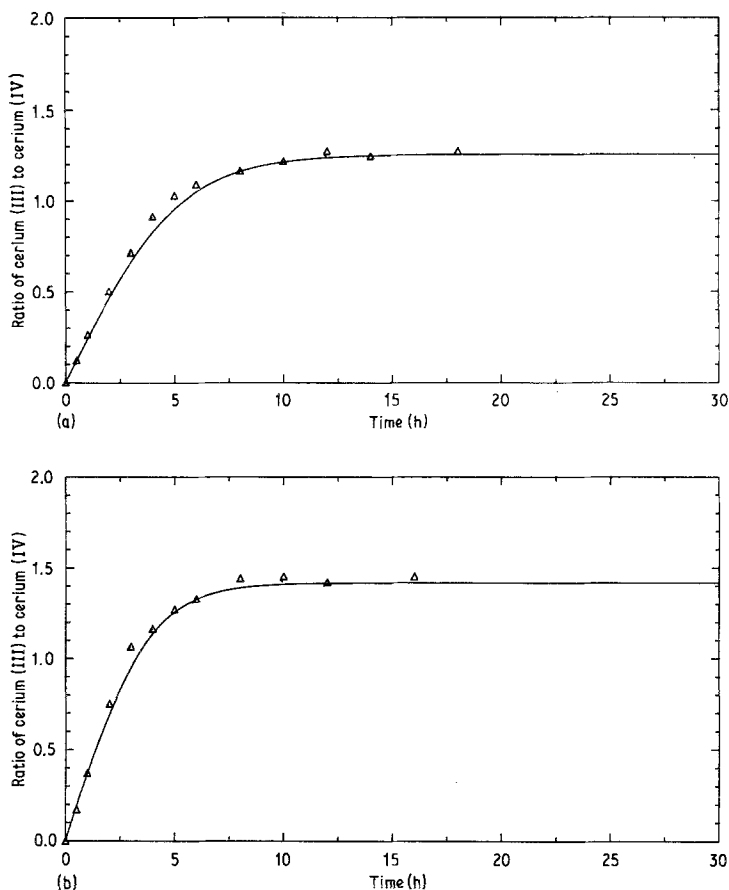


Fig. 7. Computer-generated ratio of Ce(III) to Ce(IV) versus time (solid line) and experimental data (Δ) for platinumized titanium cathode at anode current densities of (a) 50 and (b) 300 mA cm⁻² ($T = 23 \pm 1^\circ \text{C}$, $N_{\text{Re}} = 3500$).

The two parameters which most concern us are f and θ . The first of these is the true electrode area, the second the fraction of the electrode obscured by bubbles resident on the surface, thus leaving electrode area $f(1 - \theta)$ available for reaction. f can be measured directly by a number of techniques. However we do not believe that the actual surface area is the relevant parameter here.

From trials using the computer to test for the fit it was found that the best fit was obtained using the value $\theta_a = \theta_c = 0$, $f = 2$. A range of other values for θ was tested going from $\theta_a = \theta_c = 0$ to 0.5 and $\theta \neq \theta_c$ ($\theta_c = 0$, $\theta_a = 0$ to 0.4). These are shown in Table 3. Qualitatively it can be said that while it is easy to simulate the initial rapid rise in value of R with t by using $\theta_a > \theta_c$, this procedure leads to unrealistic values of R_∞ .

Mathematically identical results would be obtained using a value of $\theta_a, \theta_c = 0.5$, and $f = 4$ or indeed other combinations of f and θ such that the product $f(1 - \theta) = \text{constant}$. The choice of this value is somewhat arbitrary.

Electrode roughnesses were measured using a Rank 'Talysurf' and the values shown in Table 5 were found. It will be seen that these are smaller, but not very much so, than the predicted average diffusion layer thickness.

The effect of cathode roughness on mass transfer is shown in Fig. 2. At each of three current densities the smooth stainless steel cathode is seen to be the most effective for the reduction of Ce(IV), followed by titanium, equal to or followed by platinumized titanium and smooth platinum. This ranking is not only contrary to what one might expect but also what was found [14] in our own study of the effect of cathode texture on the rate of hypochlorite reduction. The only explanation we can offer is in terms of bubble obscuration; and Bin Yusof's [21] recent paper has shown that H_2 overvoltage was lower on smooth mild steel than on etched or bead-blasted mild steel, a surprising result which has been confirmed by Dunn [22]. This finding was explained – there seems no other ready explanation – in terms of a

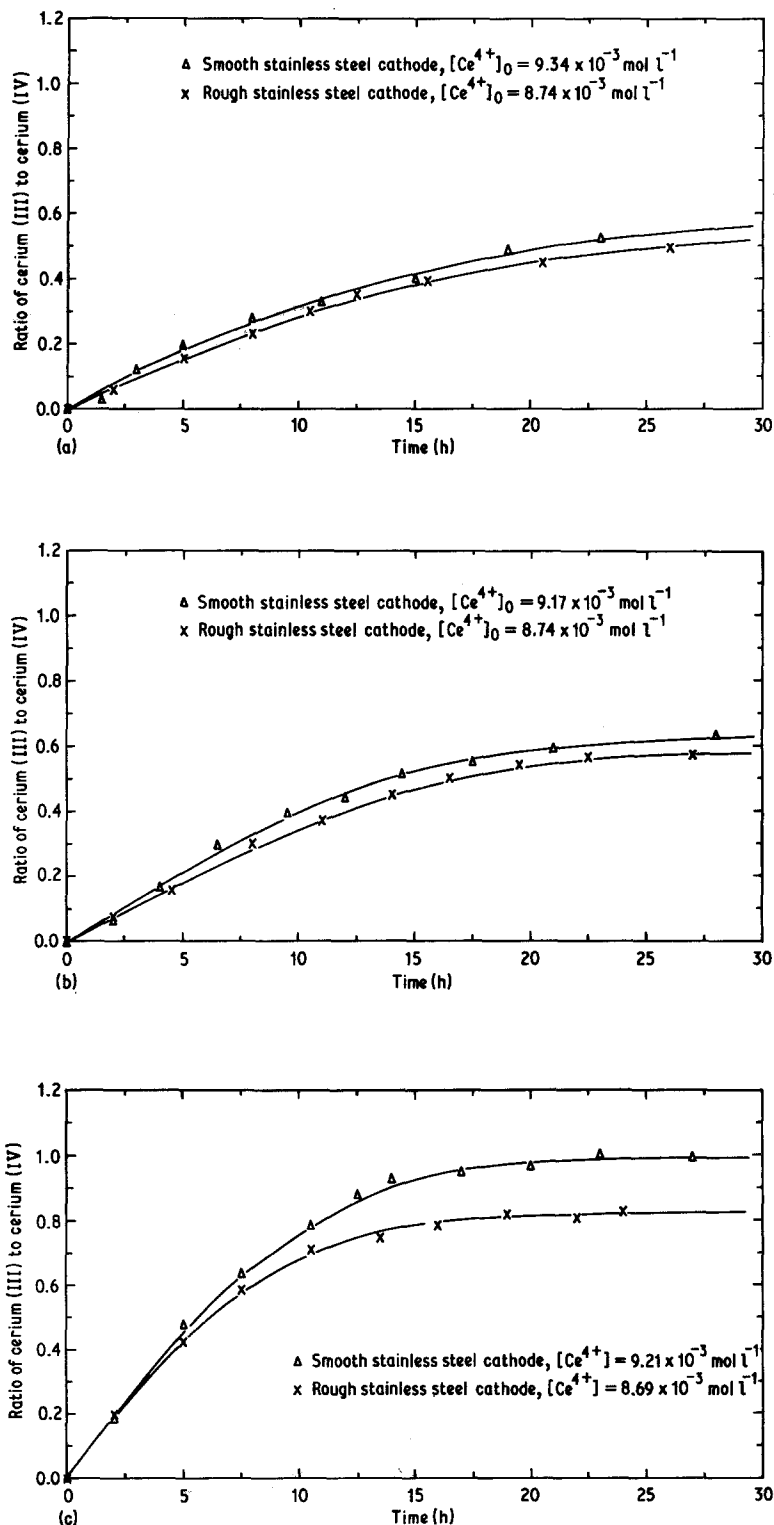


Fig. 8. Ratio of Ce(III) to Ce(IV) versus time for electrolysis of Ce^{4+} solution using smooth and rough stainless steel cathodes (A:C = 2.5:1) at anode current densities of (a) 10 mA cm^{-2} ; (b) 50 mA cm^{-2} ; and (c) 300 mA cm^{-2} ($T = 23 \pm 1^\circ \text{ C}$, $N_{Re} = 3500$).

Table 3. Table of calculated and measured R_∞ values

$A:C$	I_t (A)	Current density		Bubble obscuration*		Ratio, R_∞ ($f = 1$)	
		I_a (mA cm ⁻²)	I_c (mA cm ⁻²)	θ_a	θ_c	Measured	Calculated
0.76:1	1.0	50	38.5	0.0	0.0	1.27 (Pt/Ti)	1.30
				0.15	0.15		1.30
				0.5	0.5		1.30
	6.0	300	230.8	0.0	0.0	1.45 (Pt/Ti)	1.53
				0.25	0.25		1.53
				0.5	0.5		1.53
0.76:1	1.0	50	38.5	0.0	0.0	2.24 (stainless steel)	1.30
				0.1			1.44
				0.2			1.63
				0.3			1.86
				0.4			2.17
				0.45			2.37
	6.0	300	230.8	0.0	0.0	2.18 (stainless steel)	1.53
				0.1			1.70
				0.2			1.92
				0.3			2.19
				0.4			2.55
1.11:1	1.0	50	57.5	0.0	0.0	1.40 (stainless steel)	0.94
				0.1			1.05
				0.2			1.18
				0.3			1.35
				0.4			1.57
	6.0	300	344.8	0.0	0.0	1.08 (stainless steel)	1.16
				0.1			1.29
				0.2			1.45
				0.3			1.66
				0.4			1.93
1.8:1	1.0	50	91.7	0.0	0.0	1.10 (stainless steel)	0.65
				0.1			0.73
				0.2			0.82
				0.3			0.93
				0.4			1.09
	6.0	300	550.5	0.0	0.0	1.08 (stainless steel)	0.85
				0.1			0.94
				0.2			1.06
				0.3			1.21
				0.4			1.41

*Bubble obscuration values are trial values giving the R_∞ values in the last column.

much smaller bubble obscuration on a smooth surface than on a rough one which readily allows bubbles to 'key' into surface irregularities. It would appear that this effect outweighs that of the increased surface area which would be the result of the Talysurf measurements reported above. In the classical picture, for a diffusion-controlled reaction, differences in surface area are in any case irrelevant, as are differences in catalytic activity. However the former statement is conditional on the peak heights of the rough surface being less

than the diffusion layer. In a situation where the evolution of bubbles from the electrode surface means that, at least intermittently, the diffusion layer is vanishingly thin, one would expect an enhancement of reaction rate with a high-surface area electrode. This is the outcome of the 'penetration model' first formulated by Ibl [19]. There is too little data in the literature to enable us to do more than suggest the hypothesis that bubble obscuration on rough surfaces outweighs the benefits of increased surface area. Ibl [19] has

Table 4. Summary of values of R_∞

Anode current density (mA cm ⁻²)	R_∞ values					
	$A:C = 0.76:1$	$A:C = 1.11:1$	$A:C = 1.8:1$	$A:C = 2.5:1$	$A:C = 4.9:1$	$A:C = 10.6:1$
10	2.52	2.52	1.21	0.85	0.52	0.30
50	2.26	1.38	1.08	0.92	0.62	0.56
300	2.17	1.11	1.11	1.46	1.32	1.26

published a study in which microscopic observation was used to estimate the fraction θ of the electrode surface obscured by bubbles. We believe the values quoted by Ibl should be used as a lower figure, since there must have been other bubbles too small to be seen. However it is seen that a very satisfactory fit is obtained by us using θ values of the same order as those of Ibl and f values of about 4, although some of the electrodes used, especially Pt-Ti, will have had true f values of 30-100.

In conclusion, from the present work and also our studies on brine electrolysis in an undivided cell [14] we can confirm that back-reaction in an undivided cell can be minimized using disparate anode-to-cathode ratios. However it is seen that as current density increases and (we infer) inter-electrode gap decreases, the effect is increasingly defeated, in the case of one reaction [cerium(IV) reduction] in two different reactors, the parallel plate and concentric cylinder types (Figs. 3 and 4). In the case of the hypochlorite electrolysis, the converse is true, in that only at higher current densities is the effect of increase in anode-to-cathode ratio significant. Turning to the effect of surface roughness, we again see that there is (Fig. 8) a complete difference in the behaviour of these two systems. In the case of the hypochlorite, the expected behaviour occurs, in that the rougher surface promotes back-reaction of the hypochlorite, and this is in agreement with published literature. In the case of the cerium however, it is the smooth surfaced stainless steel that gives the

fastest reduction of Ce(IV), roughened stainless steel gives lower reduction rates than smooth stainless steel, and though the cathode over-potential on this metal was not higher on the rough than on the smooth (as found by Bin Yusof on mild steel), the difference was small and decreased with increasing current density. These voltage measurements are matched with a progressive deterioration of the performance of the rough surfaces relative to the smooth as current density increases.

However, the equally smooth Pt yields reduction rates very much slower than both stainless steel and the platinized titanium. This quartet of results gives the only possible explanation. If the effect were a catalytic one, the ranking would be:

$$\text{Pt/Ti} > \text{Pt} >$$

$$> \text{stainless steel (rough)} > \text{stainless steel (rough)} >$$

but the fact that the observed ranking is:

$$\text{stainless steel (smooth)} > \text{stainless steel (rough)} >$$

$$> \text{Pt/Ti} > \text{Pt}$$

suggests that the phenomenon must be a complex one, involving perhaps bubble size, residence time and fractional coverage. According to the penetration model of Ibl, two electrodes having identical surface areas and fractional bubble coverage would still behave differently if the residence time of bubbles on the one differed from the other. We must also recall the surprising result by Ibl and Kind [4] that surface roughness appeared to exert no effect in their studies. Here too, it is possible that bubble obscuration differences offset other factors such as surface area. From the literature on bubble formation, we know that size and behaviour of bubbles is quite different going from one metal to another. We believe that these differences provide the major explanation of our results. We acknowledge

Table 5. Electrode roughness

platinised titanium	5.0 μm
'as-received titanium'	1.0 μm
stainless steel (smooth)	0.46 μm
platinum (not measured, smoother than stainless steel)	
stainless steel (rough)	1.23 μm

Table 6. Cathode potentials (versus Hg/Hg₂SO₄)

Electrode material	Current density (mA cm ⁻²)		
	25	125	750
Smooth stainless steel	-0.93	-1.2	-1.7
Rough stainless steel	-0.76	-1.07	-1.68

that use of an undivided cell, though mechanically simpler than its divided counterpart, introduces all the complications of the back-reaction. However our confidence in the computer-based model we have been using is sufficient to assure us that these problems can be taken into account. The comparison of roughened and smooth stainless steel cathodes is particularly significant. That the effects are far less straightforward than we had imagined, encourages us to believe that optimization of the various factors described in this work will result in undivided cells operating at higher efficiencies than hitherto.

Acknowledgement

One of us (H.H.) thanks the Malaysian Government for financial support.

References

- [1] J. P. Divin, *Traitements de surfaces* Nr 126 (1973) 62.

- [2] Carus Chemical Co., US Patent no. 2843 537 (1958).
 [3] Carus Chemical Co., US Patent no. 2980 620 (1959).
 [4] N. Ibl, R. Knid and E. Adam, *Anales de Química* 71 (1975) 1008.
 [5] N. Ibl and J. Vanczel, *J. Electrochem Soc.* 113, (1966) 668.
 [6] L. J. J. Janssen and J. G. Hoogland, *Electrochim. Acta* 15 (1970) 1013.
 [7] M.G. Fouad and G. H. Sedahmed, *ibid* 17 (1972) 665.
 [8] *Idem*, *ibid* 18 (1973) 55.
 [9] M. G. Fouad, G. H. Sedahmed and H. E. El-Abd, *ibid* 18 (1973) 279.
 [10] L. J. J. Janssen and J. G. Hoogland, *ibid* 18 (1973) 543.
 [11] I. Rousar, J. Kacin, E. Lippert, F. Smirous and V. Cezner, *ibid* 20 (1975) 295.
 [12] L. J. J. Janssen, *ibid* 23 (1978) 81.
 [13] G. H. Sedahmed, *J. Appl. Electrochem.* 9 (1979) 37.
 [14] H. Hamzah and A. T. Kuhn, to be published.
 [15] G. R. Heal, A. T. Kuhn and R. B. Lartey, *J. Electrochem. Soc.* 124 (1977) 1690.
 [16] A. I. Vogel, 'A textbook of Quantitative Inorganic Analysis', 3rd ed., Longman, London (1961).
 [17] T. R. Beck, at *Electrochem. Soc. Meeting*, Cleveland, Ohio, May (1966) paper 97.
 [18] H. Vogt, *Electrochim. Acta* 23 (1978) 203.
 [19] N. Ibl and J. Venczel, *Metalloberflache* 24 (1970) 365.
 [20] Kind, PhD Thesis, ETH Zurich (1975) no. 5421.
 [21] J. Bin Yusof, A. T. Kuhn and P. Hogan, *J. Appl. Electrochem.*, in press.
 [22] P. Dunn, ICI Ltd (Mond Division), private communication.